A novel partner for *Dictyostelium* filamin is an α-helical developmentally regulated protein

Monika Knuth[1,*], Nandkumar Khaire[1,*], Adam Kuspa[2], Si Jie Lu[2], Michael Schleicher[3] and Angelika A. Noegel[1,‡]

[1]Zentrum Biochemie, Institut für Biochemie I, Medizinische Fakultät, Universität zu Köln, 50931 Köln, Germany
[2]Department of Biochemistry, Baylor College of Medicine, Houston, TX 77030, USA
[3]Institut für Zellbiologie, Ludwig-Maximilians-Universität München, Schillerstrasse 42, 80336 München, Germany
*These authors contributed equally to this work
‡Author for correspondence (e-mail: noegel@uni-koeln.de)

Accepted 16 June 2004
Journal of Cell Science 117, 5013-5022 Published by The Company of Biologists 2004
doi:10.1242/jcs.01366

Summary

The filamins are a family of highly homologous actin-crosslinking proteins that stabilize three-dimensional actin networks, link them to membrane proteins and direct intracellular signaling reactions to the actin scaffold through interaction with various binding partners. Here, we describe the first *Dictyostelium* filamin-interacting protein to be isolated – FIP, a 229.8 kDa protein with two α-helical coiled coil domains. FIP was identified in a yeast two-hybrid screen using the rod domain of filamin as bait. FIP can also be coimmunoprecipitated with filamin from cellular extracts. Deletion analysis located the interaction domain of FIP to a C-terminal region; by contrast, in filamin rods, repeats 2-4 interacted with the recombinant FIP protein. The 7 kb transcript of FIP is upregulated during early development. Monoclonal antibodies raised against a bacterially expressed FIP polypeptide recognize a 230 kDa developmentally regulated protein in western blots. Immunofluorescence analysis shows a punctate staining pattern in the cytosol and, in cell fractionation experiments, FIP is mainly found in the cytosolic fraction. A fusion protein composed of GFP and the C-terminal part localizes to the plasma membrane and is associated with the cytoskeleton. Expression of the fusion protein affects development and influences the size of the multicellular aggregates and the phototactic behavior of slugs. Thus, FIP might provide a candidate link between the dynamic actin cytoskeleton and signal transduction events during the multicellular stages of *Dictyostelium* amoebae.

Key words: ABP-120/gelation factor/ddFLN, Yeast two-hybrid system, Coiled coil structure, GFP fusion, Development

Introduction

The dynamics and three-dimensional structure of the actin cytoskeleton largely depends on the activity of different actin-binding proteins. Structures based on actin filaments range from strictly bundled parallel filaments found in microvilli or stress-fibers to loose networks as they occur in cultured cells or at the leading edge of motile *Dictyostelium discoideum* amoebae, respectively. These distinct structures can be attributed to specific activities of individual actin-crosslinking proteins or protein families like the filamins (Ayscough, 1998; Stossel et al., 2001). Structurally, filamins are dimers with large polypeptide chains that associate at their C-termini (Gorlin et al., 1990; Fucini et al., 1999). Their conserved N-terminal actin-binding domains resemble the ones of the α-actinin/spectrin superfamily of actin-binding proteins (Hartwig, 1994). The rest of the polypeptide forms 24 repeated domains of ~96 amino acids, each made up of seven antiparallel β-strands that produce an immunoglobulin fold (Fucini et al., 1997).

The *Dictyostelium* filamin (ddFLN, gelation factor, ABP-120) has a shorter elongated domain, consisting of only six 100 amino acid repeats (Noegel et al., 1989; Fucini et al., 1997). Its dimerization is mediated through the formation of intramolecular β-sheets between rod domains 6, leading to an antiparallel arrangement of the two monomer chains (McCoy et al., 1999). *Dictyostelium* mutants lacking filamin have defects in the structure of the actin cytoskeleton and exhibit reduced crosslinking of actin filaments, leading to reduced size and frequency of pseudopods. This results in a decreased motility, chemotaxis and phagocytosis of the mutant cells (Brink et al., 1990; Cox et al., 1992; Cox et al., 1995; Cox et al., 1996). In the multicellular slug stage of the amoebae, filamin deficiency causes severe defects in the orientation of the slugs during phototaxis and thermotaxis (Fisher et al., 1997).

Filamins crosslink actin filaments, promote orthogonal branching and play an important role in maintaining the cortical actin network. Apart from this, they have been reported to interact with over 30 proteins that function in diverse processes. These include integrins, sarcoglycans and transmembrane receptors such as the insulin receptor, androgen receptor and dopamine receptor D2 and D3, which control actin reorganization, nuclear transcription and neuronal signal transmission (He et al., 2003; Lin et al., 2002; Loy et al., 2003) (reviewed by Stossel et al., 2001).

A growing body of evidence points towards the involvement of filamins in the intracellular trafficking of proteins and in signal transduction. Thus, filamin influences the activity of

furin, a protease involved in the proteolytic processing of many proproteins by promoting its internalization. It also binds to a subpopulation of presenilin-1, a protein involved in early-onset familial Alzheimer's disease and in the notch signaling pathway (Stossel et al., 2001). Furthermore, it interacts with caveolin-1, a protein implicated in caveolae biogenesis, endocytic events, cholesterol transport and various signal transduction processes (Stahlhut and van Deurs, 2000). The involvement of filamin in signal transduction is inferred by its interaction with several components of the NF-κB pathway and the small GTPases RhoA, Rac1, Cdc42 and RalA (Marti et al., 1997; Otha et al., 1999). Recently, it has been reported that filamin connects the extracellular matrix to the actin cytoskeleton through migfilin, a LIM-domain-containing protein. Migfilin is recruited to cell-matrix adhesions by the cell-matrix adhesion protein mitogen-inducible gene 2 (Mig-2) (Tu et al., 2003). Loss of Mig-2 or migfilin impairs cell shape modulation. Together, Mig-2, migfilin and filamin define a connection between cell matrix adhesions and the actin cytoskeleton, and participate in the orchestration of actin assembly and cell shape modulation (Stossel and Hartwig, 2003).

Dictyostelium has emerged as a useful model to study the actin cytoskeleton and associated proteins. *Dictyostelium* amoebae possess a cytoskeleton comparable in its complexity with that of polymorphonuclear leukocytes (Devreotes and Zigmond, 1988; Noegel et al., 1997). The involvement of filamin in signal transduction pathways in *Dictyostelium* has been implicated by the photosensory and thermosensory defects of the filamin-deficient mutant (Fisher et al., 1997). To understand further the connections between the actin cytoskeleton and signal transduction, we have conducted a yeast two-hybrid screen of *Dictyostelium* cDNAs by using the elongated rod domain of filamin as 'bait'. Here, we report the first identification and characterization of a filamin-interacting protein in *Dictyostelium*, FIP. Structurally, FIP is related to large coiled coil proteins that are frequently located at intracellular membranes and are involved in protein trafficking. This relationship, combined with the fact that FIP is expressed from the very early stages of development to the formation of the fruiting body, is suggestive of an involvement of FIP in filamin-associated roles during development.

Materials and Methods

Yeast two-hybrid methods

cDNA fragments containing the complete filamin rod domain (residues 247-857) were obtained by PCR and cloned in-frame into the GAL4 DNA-binding domain (GAL4bd) vector pAS2-1 (Durfee et al., 1993). This GAL4bd-rod1-6 vector was cotransformed with a *Dictyostelium* library in which cDNAs pooled from vegetative amoebae were cloned in the pACT2 vector (Durfee et al., 1993) into the yeast strain Y190 using a method described by Gietz and Schiestl (1995). Prey plasmids were recovered from transformants that exhibited β-galactosidase activity and were tested in a cotransformation assay with GAL4bd-rod1-6 or control heterologous baits. β-galactosidase activity was determined with the nitrocellulose filter lift assay (Durfee et al., 1993). The majority of the prey plasmids that were isolated encoded the rod portion of filamin that is known to contain the dimerization site of the molecule (McCoy et al., 1999). FIP, another potential binding partner, was further characterized.

To map sites within FIP that contribute to the interaction, truncated segments of the FIP cDNA were amplified by PCR and subcloned into the pACT2 vector. In addition, full-length FIP (nucleotides 24-6234 of the published sequence (GenBank: AF356600) was cloned into pACT2 to assay its interaction with the filamin rod domain (ddFLN rod). Likewise, segments of the ddFLN rod repeats were inserted into pAS2-1. Bait and prey plasmids were simultaneously transformed into the yeast strain Y190. The involvement of the filamin rod domain 4 in binding to FIP could not be determined owing to autoactivation of this particular construct.

Expression of a FIP polypeptide and generation of monoclonal antibodies

A DNA fragment encoding the amino acids 1612-1907 of FIP was obtained by PCR using primers designed to introduce a *Nde*I site at the 5′-end and a *Sal*I site at the 3′-end. The amplified fragment was cloned into the expression vector pT7-7 (Tabor and Richardson, 1992), and the recombinant protein (rec c-FIP) expressed in *Escherichia coli* BL21. The soluble protein was purified on a Smart System (Amersham Biotech), using a Mono S cation exchange column equilibrated in TED buffer (50 mM Tris-HCl, pH 7.0, 5 mM EDTA, 5 mM DTT). The protein was eluted in a linear sodium chloride gradient at approximately 150 mM NaCl and used to immunize mice.

For mAb production, BALB/c mice were immunized with the Immune Easy mouse adjuvant (Qiagen) according to the manufacturers protocol. Spleen cells were fused with PAIB3AG81 myeloma cells 4 days after the last boost. Hybridomas were screened for their ability to recognize the antigen in enzyme-linked immunosorbent assays (ELISAs) and western blots. The monoclonal antibodies K12-349-7, K12-362-6 and K12-454-2 were used in this study. They gave identical results in western blots and immunofluorescence studies.

Expression of filamin polypeptides; in vitro and in vivo binding assays

Expression of filamin polypeptides

DNA fragments encoding G-257 to N-857 corresponding to the complete rod domain of filamin (rod 1-6), D-338 to G-657 encompassing the rod domains 2-4, and K-546 to N-857 encompassing rod 4-6 were obtained by PCR, sequenced and cloned into the expression vector pT7-7. Recombinant proteins were expressed in *E. coli* K38 or BL21. All proteins were soluble. For purification of rod 1-6, anion exchange chromatography (DE52 cellulose; Whatman) followed by gel filtration (Sephacryl S-300; Amersham Biotech) in IEDNBP buffer, pH 7.6 (10 mM imidazole, 1 mM EGTA, 1 mM DTT, 200 mM NaCl, 1 mM benzamidine, 1 mM PMSF) was performed. Rod 3, rod 4, rod 2-4, rod 4-6 and rod 5-6 (Fucini et al., 1997; Fucini et al., 1999) were purified using anion exchange chromatography followed by hydrophobic interaction chromatography with Phenyl-Sepharose (Amersham Biotech). The proteins were eluted in a linear 1.7 M-0 M ammonium sulfate gradient in 100 mM sodium phosphate, pH 7.0.

ELISAs

96-well maxisorb plates (Life Technologies) were coated overnight at 4°C with recombinant rod polypeptides or an unrelated GST-fusion protein at 20 μg/ml. The wells were washed three times with PBS containing 0.05% Triton X-100 (PBS/TX100) and blocked with PBS containing 1% BSA (PBS/BSA) for 2 hours at 20°C. Following three washes with PBS/TX100, the wells were incubated with the indicated concentrations of FIP recombinant polypeptide diluted in PBS/BSA for 2 hours at 20°C. The wells were washed six times with PBS/TX100 and then incubated with FIP-specific mAb K12-454-2

for 1 hour at 20°C. After washing six times with PBS/TX100, incubation with alkaline phosphatase-conjugated goat anti-mouse IgG (Sigma Aldrich) diluted 1:10,000 in PBS/TX100 was performed at 20°C for 1 hour, followed by six washing steps with PBS/TX100 and treatment with a *p*-nitrophenylphosphate solution (Sigma Fast tablets; Sigma Aldrich) for 30 minutes at 20°C. The optical density was measured using an ELISA plate reader (Labsystems) at a wavelength of 405 nm.

Immunoprecipitation assays

Mixtures of recombinant FIP and various filamin rod polypeptides (30 μg each) were incubated for 15 minutes at 4°C in IP buffer (50 mM Tris-HCl, pH 8.0, 70 mM NaCl, 1% Triton X-100, 1% BSA). The solutions were incubated with FIP-specific mAb K12-454-2 for 1 hour at 4°C. Immune complexes were recovered by addition of 50 μl protein A-Sepharose beads (Amersham Biotech), electrophoresed on SDS-polyacrylamide gels, and stained with Coomassie Blue.

For the analysis of the in vivo interaction, AX2 wild-type cells or cells expressing the GFP-tagged FIP C-terminus were lysed by sonication and the solution adjusted to 1× IP buffer (100 mM potassium phosphate, pH 7.9, 75 mM NaCl, 5 mM EDTA, 1 mM benzamidine, 0.5 mM PMSF) in the presence of 0.1% Triton X-100. Immunoprecipitation was carried out with the FIP-specific mAb K12-454-2, GFP-specific mAb K3-184-2 (Noegel et al., 2004) or the filamin-specific mAb 82-454-12 (Brink et al., 1990). The immunoprecipitates were tested for the presence of filamin or FIP or the GFP fusion protein by western blot analysis.

Strains, growth conditions and development of *D. discoideum*

Cells of *D. discoideum* strain AX2-214 (referred to as wild-type), transformants and the filamin-deficient mutant GHR (Fisher et al., 1997) or HG1264 (Brink et al., 1990) were grown either in liquid nutrient medium at 21°C with shaking at 160 rpm (Claviez et al., 1982), or on SM agar plates with *Klebsiella aerogenes* (Williams and Newell, 1976). For development, cells were grown to a density of 2-3×10^6 cells/ml, washed in 17 mM Soerensen phosphate buffer, pH 6.0, and 1×10^8 cells were deposited on phosphate agar plates and allowed to develop at 21°C as described (Newell et al., 1969). Images of aggregates and fruiting bodies were taken with a Leica MZ FLIII microscope and processed using the Diskus 4.20 software (Hilgers). Alternatively, development was by shaking in suspension in Soerensen phosphate buffer at a density of 1×10^7 cells/ml.

Phototaxis analysis

To analyze slug behavior, 5×10^6 amoebae were inoculated onto a circular, 0.5 cm^2 origin at the center of a water agar plate. Slugs were allowed to form and migrate towards light (Fisher et al., 1997). After 48 hours, slugs and slime trails were transferred to nitrocellulose filters (BA85, Schleicher and Schuell) and stained with Amido Black.

Western, Southern and northern blotting

SDS-PAGE and western blotting were performed essentially as described previously (Laemmli, 1970; Towbin et al., 1979). Nitrocellulose (BA 85; Schleicher and Schuell) was used as a blotting matrix. Primary antibodies were detected with HRP-conjugated goat anti-mouse antibodies followed by chemiluminescence. DNA and RNA were isolated as described (Noegel et al., 1985), transferred onto nylon membranes (Biodyne B; Pall Filtron) and incubated with ^{32}P-labeled probes generated using a random prime labeling kit (Stratagene). Hybridization was performed at 37°C for 12-16 hours in hybridization buffer containing 50% formamide and 2× SSC. The blots were washed twice for 30 minutes in a buffer containing 50% formamide, 0.2% SDS and 2× SSC at 37°C.

Cloning and expression of GFP-FIP fusion proteins

Vectors were constructed that allowed expression of green fluorescent protein (GFP) fused to full-length FIP and a C-terminal fragment of FIP in AX2 cells. Expression was under the control of the actin-15 promoter and the actin-8 terminator. The cDNA fragment isolated from pACT2 was cloned in-frame at its 5′-end to the coding region of the red shifted S65T mutant of *Aequoria victoria* GFP in the transformation vector pDEX-GFP (Westphal et al., 1997). The continuous reading frame was composed of GFP, the peptide linker KLELIRHE resulting from the cloning strategy, and a FIP fragment from Glu1163 to Lys2038. For expression of full-length FIP as a GFP fusion protein, the full-length cDNA was cloned into the pDEX-GFP vector. The vectors were introduced into AX2 cells by electroporation. After selection for growth in the presence of G418 (Sigma Aldrich), GFP-expressing transformants were confirmed by visual inspection under a fluorescence microscope.

Fluorescence microscopy

Cells were fixed either in cold methanol (–20°C) or at room temperature with picric acid/paraformaldehyde (15% vol/vol of a saturated aqueous solution of pricric acid/2% paraformaldehyde, pH 6.0) followed by 70% ethanol. For studies on developed cells, multicellular structures were disaggregated by passage through a 23-G needle before fixation. For studies of cytoskeletal rearrangements, the cells were incubated with 20 μM cytochalasin A or 50 μM 2,4-dinitrophenol in 17 mM Soerensen phosphate buffer, pH 6.0, for 1 hour prior to fixation. DMSO treatment was done as described (Weiner et al., 1993). FIP was detected using mAb K12-362-8 or K12-454-2, filamin using mAb 82-382-8 or 82-454-12 as well as a polyclonal antiserum (Brink et al., 1990), GFP fusion proteins using GFP-specific monoclonal antibody K3-184-2 (Noegel et al., 2004) and actin using mAb Act1-7 (Simpson et al., 1984) followed by incubation with Alexa488- or Cy3-labeled goat anti-mouse IgG secondary antibody or Alexa568-labeled goat anti-rabbit IgG secondary antibody (Molecular Probes, Sigma Aldrich).

For phagocytosis studies, GFP-cFIP-expressing AX2 cells were plated on coverslips and incubated with 1×10^6 TRITC-labeled YSC yeast cells and observed by fluorescence microscopy. Confocal images were taken with an inverted Leica TCS-SP laser-scanning microscope with a 63× PL Fluotar 1.32-0.6 oil immersion objective. The 488 nm argon ion laser line was used for excitation of GFP and the 568 nm krypton ion laser line was used for excitation of the Cy3 fluorophor. Images were processed using the accompanying software.

Cell fractionation experiments

2×10^8 cells were allowed to develop for 15 hours on phosphate agar plates. Multicellular structures were washed off the plates, disaggregated and lysed in cold homogenization buffer (50 mM Tris-HCl, pH 7.4, 5 mM DTT, 5 mM EDTA) with a protease inhibitor cocktail (Roche Diagnostics) by repeated passage through 5 μm Nuclepore filters (Corning Costar) or by freezing and thawing. Cytosolic and membrane (including nuclei) fractions were separated by centrifugation at 10,000 ***g***, the supernatant was further fractionated by ultracentrifugation at 100,000 ***g*** for 1 hour at 4°C. Proteins were separated by SDS-PAGE (8% or 10% acrylamide) and the resulting western blot probed for FIP and filamin.

Miscellaneous methods

ddFLN purification and actin isolation were done as described (Brink et al., 1990). Low-shear viscometry measurements were done in the presence or absence of recombinant FIP polypeptide (Eichinger and Schleicher, 1992).

Results

Identification, sequence and structural features of a novel filamin-binding protein

In order to identify binding partners for *Dictyostelium* filamin we have performed a yeast two-hybrid screen using the rod portion of filamin as bait. Among the clones was a 1.8 kb cDNA coding for residues 281-857 of filamin, confirming our previous findings that filamin dimerizes through its rod domain (Fucini et al., 1999; McCoy et al., 1999). A 2.6 kb cDNA coded for the C-terminal part of a novel protein that we called filamin-interacting protein (FIP).

The full-length 6234 bp cDNA was assembled from a λ-ZAP library. This DNA included a 5′-untranslated region of 23 bp and a 3′-untranslated region of 96 bp with a polyadenylation signal and a polyA tail (GenBank: AF356600). Sequence comparison with the *D. discoideum* genome database (http://www.uni-koeln.de/dictyostelium/) revealed the existence of two introns in the genomic sequence. The *ddfip* gene is located on chromosome 2.

The ddFIP cDNA encodes a protein composed of 2038 amino acids, with a calculated molecular mass of 229,799 Da (Fig. 1A). Predictions of secondary structure provided by the COILS algorithm (Lupas et al., 1991) define the presence of two α-helical coiled coil domains between amino acids 603-904 and 1217-1733, respectively. These domains consist of α-helical structures with a length of 20-100 amino acids interrupted by short stretches of 5-25 amino acids with random conformation. The very beginning and the end of the FIP sequence harbor a predicted leucine-zipper motive (boxed in Fig. 1A). Database searches revealed only weak homologies of the predicted coiled coil domains (19-22% identity, up to 42% similarity) to entries corresponding to proteins known to have α-helical structures, like tail sequences of myosins or *Dictyostelium* interaptin (Rivero et al., 1998), golgin-245 (Griffith et al., 1997) or the yeast cytoskeleton-related protein USO1 (Nakajima et al., 1991), indicating a structural analogy between these proteins. Monoclonal antibodies raised against a C-terminally derived polypeptide (amino acids 1612-1907) recognized a single protein of approximately 230 kDa in western blots, which is well in agreement with the predicted molecular mass of FIP (Fig. 1B).

Developmental regulation of FIP

The 7 kb FIP transcript is present at very low levels during growth phase (Fig. 2A). The mRNA accumulates during early development and stays at a high level during the following differentiation stages (t_{10}-t_{16}), when prespore and prestalk cells form and sort out. Expression of the 7 kb transcript decreases to basal levels during the maturation of the fruiting body. The protein is hardly detectable in growth phase cells, but the amount increases during early development, reaches a maximum at 12 hours of starvation, and is maintained during migration, culmination and the maturation of the fruiting body (Fig. 2B).

Subcellular localization of FIP

In cells starved for 9 hours in shaking suspension as well as in cells that were developed for 15 hours on phosphate agar plates, FIP is present in the cytosol mainly in a punctate fashion. Methanol or picric acid/paraformaldehyde fixation gave comparable results. In *Dictyostelium* filamin-deficient mutant strains, the distribution of FIP was as in wild-type, implying that the intracellular localization of FIP is not strictly dependent on its binding partner filamin (data not shown).

Filamin shows a different distribution. In methanol-fixed cells, it is found around the periphery of the cell and also

A

```
MLEQLSENVS QLILTVLELK DKNANLPVVE VTAIANAASS ISDIAIKLAD     50
AEYSNYPSIY NEIINTTTNM STIKKTTIDC IANFQTTTNK QLSWSNLIQS    100
CKNIANETYK ILKVIYDADI KRLKHLIETC KNQFKNNENS FGMIDREEFN    150
GFGELVNQTI SNLIEYSSCL EVKAKENQLS SPLQNQFIDD DDDDIIKLSQ    200
QLVEDANRLI DIVNDIFSDL DDPSQKQKFI NHQNSLLNQL NHTFNLIQTN    250
SPTLSLPEFT NVNNYIQSPI PSQYSTSNIK TIYNDNNNSN NNNNNNSIEI    300
NNEINNNNNI DKNENNNLLN DLIRGISKSC IEELRAACRG DPMATETISN    350
SIQQLIPILN DTLNQHIKNN NNINKNEKEI LEKSINKLKN DLIQKYIQSA    400
TLVTRSSGNQ NVKNDEINKM IEGLESIQDC LNSIDGIVST KEDQFLNAIK    450
AKEDVLTILS DHSIANNTQA IVGTLKHLAK NQHQIEALIT STSTTPDDDN    500
NNNNNSSINP EINEAVSKLS ELLPLQIQAA KLYLKDSTNL ENRKQFTDIS    550
NSMKLPLSKI QSLMEPSTIS DSNELLSKQE NSSNQVLLNN INNNSNNNNN    600
NNIEENSKLI DKLLKDLEND NANLVGLIES ELVLSNDTLL KEFVKKTIDQ    650
LLKEVQNRRD IGMNKFSKSP FDKDVKQEFL KSNQLISDLS KSLIDCLKSF    700
EVVPLLKLQL LNCHPQSVTP NSPKLQSTQK DINNRINSII YNYKDQMLDQ    750
PLIENQIKQL ESYQNQLNQE LSKDLNGSKD NLSYILDNII NNISNLSNLP    800
SSSTNDGDGG GRQVIIPIEN LNDEIIDGIN EEINKEIIKE NKENEIKRDN    850
ERLEELKQLE NLSNDQKLLK LFNDLIQYLK NNEANKSVVT LKQLIGEQDK    900
LIQLGNEIKQ NSNSQDFKDQ IDSSINLFKN SISSSIALAG KTAKINDDPQ    950
LTKACKTVKK SIIELTRLLK LNPLIEELSS YQQALLLKPH PINENIIKGF   1000
KEHQINSRYY IETAYQVGKD DLISQSIEKI VYQQSELLKL ASNHLTSKEV   1050
SETLDPNIQL LLANSLETVK KSIVDQVEAA LSFLESEKSD DQIEKLLTIL   1100
DTVSESVDNC SKSIFFATGK GKQQQDLSPT TISQNTIKQS INSIIPTLTL   1150
QATQLQSNPN DKELEKKHQQ LLDQIIQPLE QLILNPNINQ IIDKENIENN   1200
NNNNNNDNNN NNDDDDEEE DKKIKKLIND EKKELDKLES NALDSDSKGV   1250
VESSRSLVKL HQEILSLADS LTSSTAVLID ANQNNADFER NLIIKECSKE   1300
LSTLIPLQLQ TIKSMLQSKD IPTEASYQKK VGFINNQIKR NLNEIEKQSS   1350
NNNSNYKLIS KTPYYSDQFK KLSNKIDNNG MLIKDENQFK VNLKRLEKLA   1400
GKCIDSSNFD LSRQQSYLDK ERQQRIRDAI NKLENKLNGK NNDSTDDLSN   1450
KINQYLKQPL NPISREQFEK VRSQFQQTLD NLINEQLSTP LQLLLNHSNL   1500
IQKLSRQSTQ QPINNNNNAN NNVKIQETTK KILENYSKLK QQLINNDIKL   1550
NESKKLIIGK SLKEIETLTP QLIVASNNCL NDNNNDQKKR ELLENLQTKI   1600
ESPIYEILNQ LDSIDPIFQF KNAIKQYQAT LIKLNDSIDV STVTNDNSKQ   1650
IDEYISKLSN LQSNHLIPLL KQQGLNEKEL KEFESQLKSK LSDVNSISKD   1700
YLKNLKQSKL TDTIKAEKDM SISSLCNLIN SIQSINQPKI EDNRIKLSQS   1750
SQSKSKDIKQ LVDSIKSNNL LPIVESPNKI ERYVSIQTNS TKPIFSSSSS   1800
NNGKIISTAQ VNYKPRSSSQ PQKPILTNTN NITITKPIRP IETRVPIKLT   1850
TQPQSTNPKT VPPTTTTTTE ATTTATKPIP NKTPQPINTF KPSDKGASLE   1900
DSCINAANQM SNISGNEQLG TIGKELEAYA NAIKIGDKKQ ILLCGRNISI   1950
LLNKYSTEVS NNIKSTPTSN KMLQTRCSHG IGVLQTLSCQ FKILSSVKAA   2000
SDEKDSDSDS QLTSMVNQLT STLLDLNTST STLNKFKK               2038
```

B

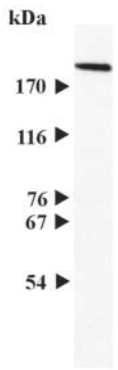

Fig. 1. The FIP cDNA codes for a 230 kDa protein. (A) The sequence predicts a protein of 229.8 kDa. The predicted coiled coil domains are underlined. The two leucine-zipper motives are boxed and the filamin-binding region is double boxed. These sequence data are available from GenBank/EMBL/DDJB under accession number AF356600. (B) mAb K12-454-2 recognizes a 230 kDa protein in protein extracts from developing AX2 cells (t6).

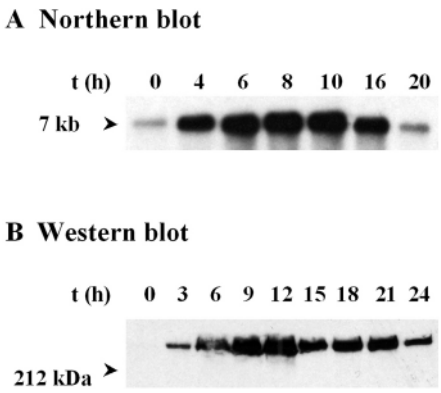

Fig. 2. The presence of ddFIP mRNA and protein during development. *Dictyostelium* amoebae of strain AX2 were starved on phosphate agar. At the indicated time points, samples were taken for RNA extraction or preparation of total cell homogenates. (A) RNA blots containing 30 μg of total RNA per lane were probed with a 2.7 kb fragment encompassing the 5′-end of the FIP DNA. Transcript levels are rising during the early developmental stages and are maintained throughout culmination. During maturation of the fruiting body, the transcript level decreases. (B) Total cell homogenates of 1×10^6 cells per lane were resolved in 8% polyacrylamide gels and blotted onto nitrocellulose membranes. Blots were incubated with mAb K12-454-2. The antibody recognizes a 230 kDa band throughout all stages of development.

throughout the cytosol in a more homogeneous fashion. However, when we carefully examined coimmunofluorescence pictures obtained with polyclonal filamin antibodies and monoclonal FIP-specific antibodies, we noted a colocalization of both proteins in cell-to-cell adhesion zones of aggregating cells (Fig. 3). In cells that had been transformed with a vector allowing expression of a GFP-tagged full-length FIP, expression of the fusion protein was very low and could only be detected by immunofluorescence using GFP-specific mAB K3-184-2. The pattern of GFP-FIP distribution was similar to the pattern of the endogenous protein (data not shown).

When subcellular fractions obtained by centrifugation were assayed for FIP distribution, we found FIP mainly in the soluble fraction, whereas a minor population was detected in the 10,000 ***g*** pellet. Upon further fractionation of the 10,000 ***g*** supernatant at 100,000 ***g***, a faint band was seen in the 100,000 ***g*** pellet; however, the majority of the protein was present in the supernatant. Filamin showed a similar behavior (Fig. 4A). To confirm the interaction further between filamin and FIP, we performed coimmunoprecipitation experiments using whole cell lysates. We could immunoprecipitate FIP with the filamin-specific mAB 82-454-2; conversely, the FIP antibody K12-454-2 coimmunoprecipitated filamin (Fig. 4B). The filters were reprobed for the presence of the respective antigens (data not shown).

Mapping of filamin-FIP interaction domains and assaying the specificity of the interaction

To define precisely the minimal FIP and filamin protein fragments required for the productive interaction of both proteins, we prepared a series of cDNA constructs containing different fragments of each of these two proteins and examined their ability to interact using the yeast two-hybrid system (data not shown). In this way, the interaction site in FIP was located to amino acids 1719-1826, a rather serine-rich stretch adjacent to the coiled coil domain (see Fig. 1A, double boxed sequence). To narrow down the filamin interaction site, we used biochemical assays. We first examined the ability of recombinant filamin polypeptide rod 1-6 to bind to a recombinant FIP polypeptide (rec c-FIP: residues 1612-1907) containing the filamin-binding domain using an ELISA. In this assay, the interaction between the FIP polypeptide and filamin rod 1-6 that was detected with the mAb 82-382-8 was specific and saturable, and was not blocked by the addition of 0.5% bovine serum albumin. The assay worked in both directions, either with rod 1-6 binding to preadsorbed FIP polypeptide or vice versa (data not shown). We then used recombinant rod polypeptides representing rod 3, rod 4, rod 2-4, rod 4-6 and rod 5-6 to narrow down the binding site in filamin. In this assay, the FIP polypeptide showed a specific and saturable binding to rod 2-4, whereas the other rod portions showed weaker interactions, with rod 3 and rod 5-6 giving the lowest values. An unrelated polypeptide was used for control (Fig. 5A). The

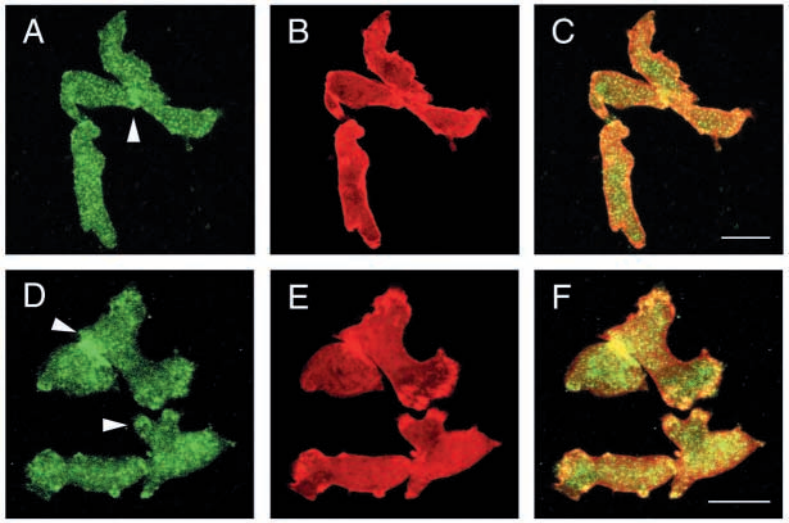

Fig. 3. Colocalization of FIP with filamin in aggregating AX2 cells as analyzed by confocal microscopy. Cells were starved for 10 hours in shaking suspension, fixed with methanol and stained with FIP-specific mAb K12-362-8 (A) or K12-454-2 (D) and a polyclonal filamin serum (B,E). C and F show the overlays. Detection was with Alexa488-conjugated goat anti-mouse IgG and Alexa568-labeled goat anti-rabbit IgG. The arrows point to areas of colocalization. Bar, 10 μm.

rod 2-4 interaction with FIP was further confirmed by coimmunoprecipitation experiments where we mixed the FIP polypeptide with rod 2-4, rod 5-6, rod 3 and rod 4, and precipitated the proteins with mAb K12-454-2. In this assay, only rod 2-4 coprecipitated with c-FIP. The binding was specific and depended on the presence of the FIP polypeptide in the assay (Fig. 5B). We conclude that the FIP polypeptide binds tightly to the rod portion of filamin. However, this binding does not affect the crosslinking activity of ddFLN with F-actin in vitro. When we added FIP polypeptide in low shear viscometry measurements to the assay mixture, the viscosity of the F-actin solution was comparable with controls where only ddFLN had been added (data not shown).

C-terminal FIP sequences mediate membrane localization

To investigate further the association of FIP with filamin and the actin cytoskeleton in *D. discoideum*, we fused GFP to the C-terminal 2.7 kb fragment of FIP encompassing residues 1163-2038, which contains the filamin-binding site. The actin-

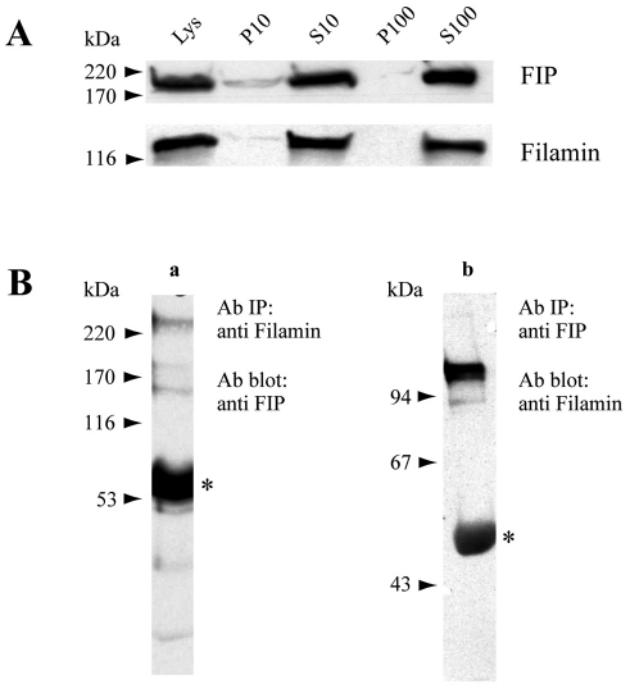

Fig. 4. FIP distribution in cell fractionation experiments and coimmunoprecipitation of filamin and FIP. (A) 2×10^8 AX2 cells were developed for 15 hours on phosphate agar, opened by freezing and thawing (Lys), and cytoplasm and membrane fractions were separated by centrifugation at 10,000 ***g*** into supernatant (S10) and pellet (P10). The supernatant (S10) was further fractionated by centrifugation at 100,000 ***g*** into supernatant (S100) and pellet (P100). The fractions were resolved in 8% polyacrylamide SDS gels and blotted onto nitrocellulose membranes. Blots were incubated with mAb K12-454-2 for FIP detection and filamin-specific mAb 82-454-12. Both proteins are mostly present in the cytosolic fraction and to a lesser extent in the membrane sediment. (B) FIP (a) and filamin (b) can be coimmunoprecipitated from AX2 cell homogenates. In (a), immunoprecipitation was performed with filamin-specific mAb 82-454-12, and the immunoblot containing the immunocomplexes was probed for the presence of FIP with mAb K12-454-2. In (b), immunoprecipitation was performed with FIP-specific mAb K12-454-2, and filamin was detected in the immunoprecipitate using mAb 82-454-12. The immunocomplexes were resolved by SDS-PAGE (10% acrylamide). The bands observed at approximately 170 kDa in (a) are breakdown products of FIP. Likewise, the band below 94 kDa in (b) is a breakdown product of filamin. Both proteins are highly susceptible to proteolysis. The bands at about 60 kDa (star) are the immunoglobulin heavy chains. The homogenates were obtained from cells that were allowed to develop on phosphate agar plates for 12 hours.

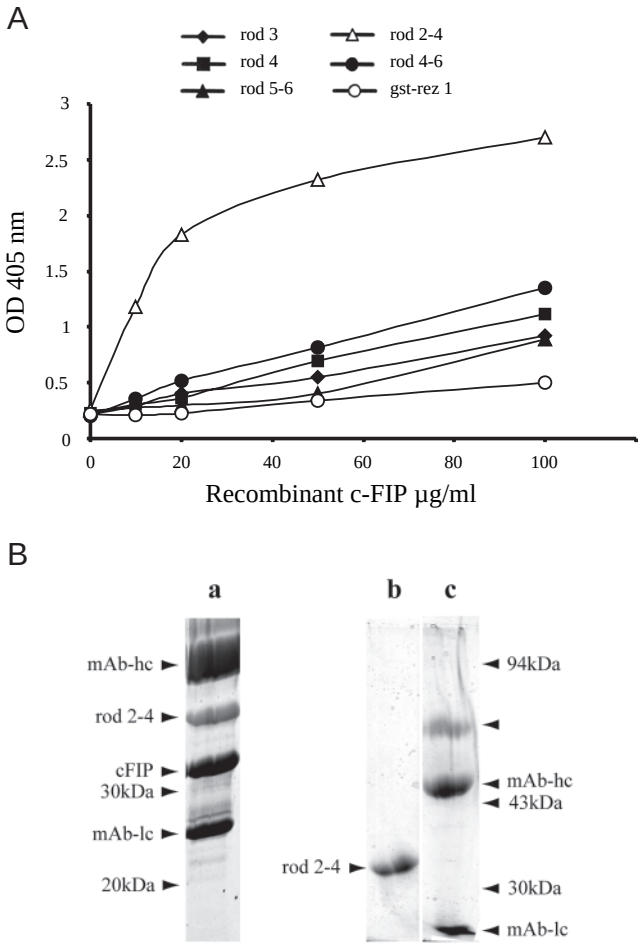

Fig. 5. Verification of the filamin-FIP interaction. (A) 20 µg/ml each of filamin rod polypeptides rod 3, rod 4, rod 5-6, rod 2-4, rod 4-6 and an unrelated polypeptide (gst-rez 1) were immobilized on plastic and increasing amounts of FIP polypeptide (rec c-FIP; residues 1612-1907) were added. The ability of the rod proteins to bind the recombinant FIP polypeptide was measured by ELISA using mAb K12-454-2. Measurements were performed in duplicate. Data from a representative experiment are shown. (B) Direct interaction of FIP polypeptide and rod 2-4. Both polypeptides (30 µg each) were mixed and immunoprecipitation was performed using mAb K12-454-2. The immunoprecipitate was resolved by SDS-PAGE (12% acrylamide) and stained with Coomassie Blue (a). The control in c shows that rod 2-4 polypeptide (see b) is not precipitated by mAb K12-454-2 in the absence of the FIP polypeptide. The proteins were separated by SDS-PAGE (10% acrylamide). The location of the molecular weight markers as well as of the immunoglobulin light (lc) and heavy chain (hc) is indicated by arrows. The band at approximately 70 kDa also represents the antibody.

15 promoter allowed constitutive expression of the fusion protein, which we called GFP-cFIP for brevity. The amount of the GFP-cFIP fusion protein in the cells is approximately twice as high as that of the endogenous FIP during development (data not shown). GFP-cFIP-expressing AX2 cells display a prominent plasma membrane staining along with a punctate staining in the cytoplasm. During phagocytosis of yeast cells, the GFP-cFIP fusion protein is present at the plasma membrane during formation of the pseudopodia surrounding the particle and during the closure of the phagocytic cup (Fig. 6A). The fluorescence disappears after the ingestion of the phagosome. GFP-cFIP is released once the particle is ingested. Likewise, GFP-cFIP accumulated on particles undergoing exocytosis (Fig. 6B). The plasma membrane localization of GFP-cFIP coincides with the one of filamin. Moreover, GFP-tagged filamin behaves similarly during phagocytosis of yeast particles (data not shown). At the biochemical level, GFP-cFIP could be efficiently coimmunoprecipitated with filamin (data not shown).

Cytoskeletal rearrangements affect GFP-cFIP

Upon treatment with cytochalasin A, the GFP-cFIP fluorescence at the plasma membrane is disrupted and resembles the filamin distribution, with which it partly overlaps (Fig. 7A). When using an actin-specific monoclonal antibody, we observed a fragmentation of the cortical actin. GFP-cFIP mostly colocalized with actin (Fig. 7B). We also tested the effect of 2,4-dinitrophenol (DNP), an uncoupling agent of the oxidative phosphorylation that disturbs the actin cytoskeleton (Jungbluth et al., 1994), and found that GFP-cFIP redistributed in a similar way (data not shown). This is a further indication of the association of GFP-cFIP with the cortical actin cytoskeleton. This association may be partly, but not exclusively, mediated by its interaction with filamin. We have also studied an association of the endogenous FIP with the actin cytoskeleton by treating cells with DMSO, which leads to a rapid disassembly of the actin cytoskeleton and the formation of new actin structures in the cytoplasm. Along with these changes, FIP also changed its distribution and was more concentrated in spots of varying sizes as compared with the dotted staining pattern in untreated cells (data not shown).

Expression of GFP-cFIP affects development and phototaxis

When analyzing GFP-cFIP-expressing cells, we observed that they finished the developmental program earlier than AX2 cells. AX2 cells develop fruiting bodies approximately 24 hours after the onset of starvation, whereas GFP-cFIP cells need only 16 hours to complete development (Fig. 8A). Furthermore, the expression of the GFP-cFIP fusion protein leads to the formation of smaller aggregates, which develop into shorter fruiting bodies than wild-type. The diameter of the aggregates and the length of the fruiting bodies is reduced by 30% in the GFP-cFIP-expressing cell line (Fig. 8B). From this, we conclude that the expression of a truncated form of FIP interferes with proper developmental timing.

The lack of filamin leads to a phototaxis defect in AX2 cells (Fisher et al., 1997; Wallraff and Wallraff, 1997). Therefore,

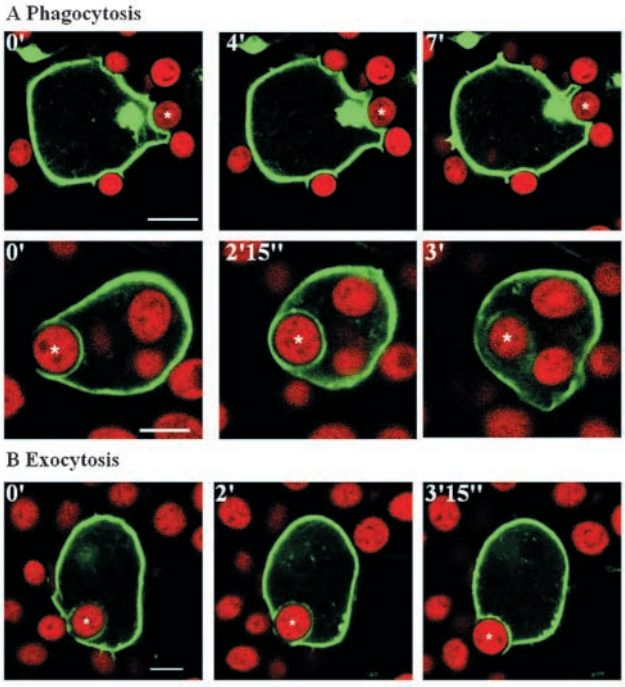

Fig. 6. Localization of the GFP-cFIP fusion protein during phagocytosis and exocytosis. Single confocal sections through living AX2 cells expressing the GFP-cFIP fusion protein. (A) Uptake of TRITC-labeled yeast cells (indicated by a star). GFP-cFIP is located at the plasma membrane during the formation (upper panel) and the engulfment of the phagosome (lower panel). GFP-cFIP is released from the phagosomal membrane after complete engulfment of the yeast particle. (B) GFP-cFIP reassembles at the membrane during exocytosis of TRITC-labeled yeast cells. Bar, 5 μm.

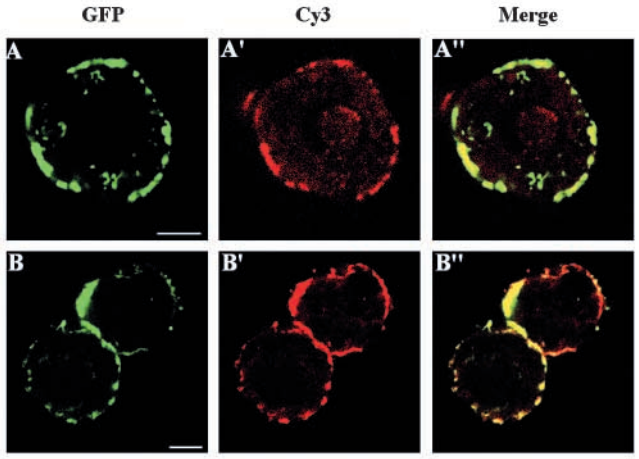

Fig. 7. Cytoskeletal association of the GFP-cFIP fusion protein during cytoskeletal rearrangements in response to cytochalasin A. *Dictyostelium* AX2 cells expressing the GFP-cFIP fusion protein were attached to coverslips and treated with 20 μM cytochalasin A in phosphate buffer for 1 hour prior to fixation with methanol. In the upper panel, a cell labeled with the filamin-specific mAb 82-382-8 and, in the lower panel, a cell stained with the actin-specific mAb Act 1-7 is shown (A,B, GFP fluorescence; A',B', antibody staining; A'',B'', overlay). The merged pictures (A'',B'') reveal a cytoskeletal association of the GFP-cFIP fusion protein. It colocalizes with the cytoskeletal elements in patches at the plasma membrane. Bar, 5 μm.

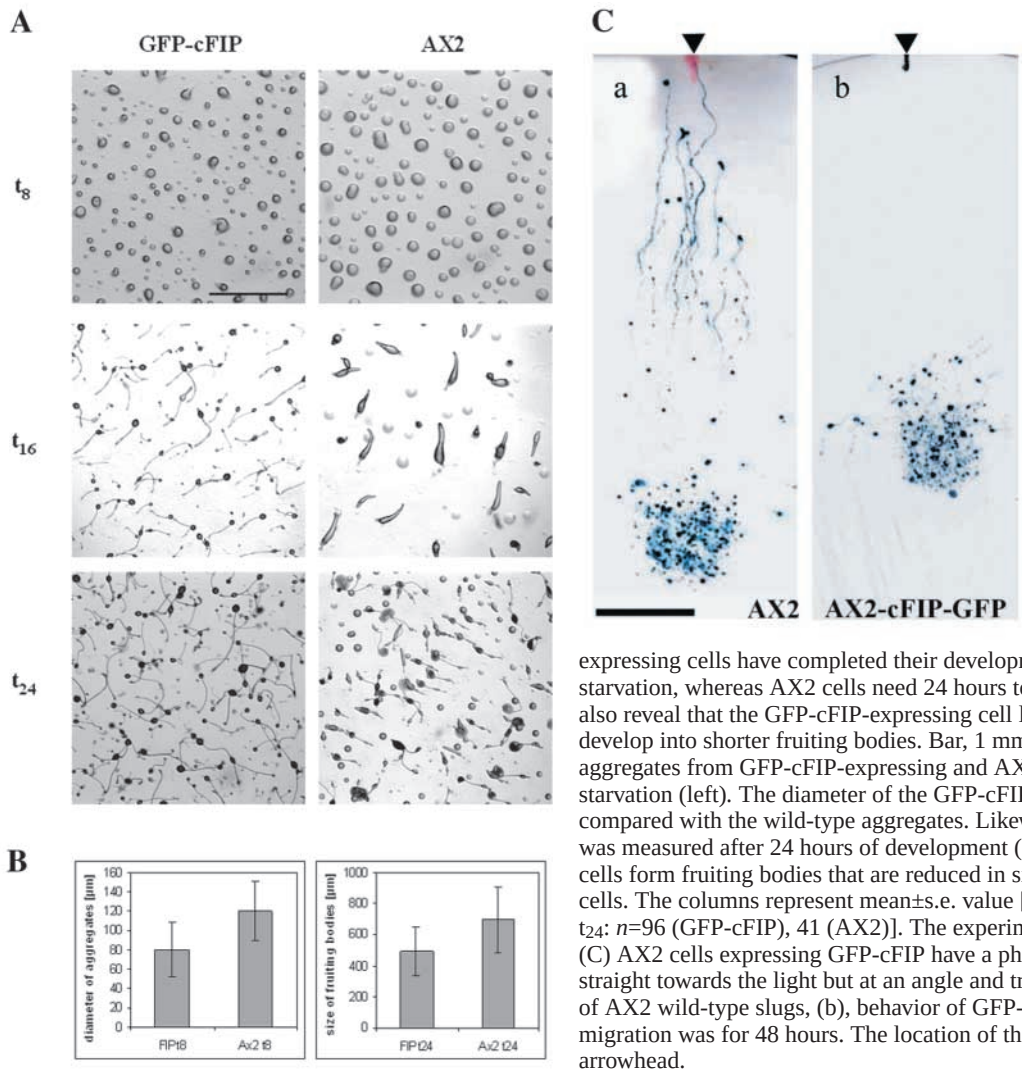

Fig. 8. Expression of GFP-cFIP in AX2 affects development and phototaxis. (A) 1×10^8 cells were deposited onto a phosphate agar plate, allowed to developed at 21°C and documented at the indicated times. (A) Microscopic images of the developmental stages of GFP-cFIP-expressing cells and AX2 cells at the indicated time points. GFP-cFIP-expressing cells have completed their developmental program after 16 hours of starvation, whereas AX2 cells need 24 hours to form fruiting bodies. The figures also reveal that the GFP-cFIP-expressing cell line forms smaller aggregates that develop into shorter fruiting bodies. Bar, 1 mm. (B) Differences in the size of the aggregates from GFP-cFIP-expressing and AX2 cells measured after 8 hours of starvation (left). The diameter of the GFP-cFIP aggregates is reduced by about 30% compared with the wild-type aggregates. Likewise, the length of the fruiting bodies was measured after 24 hours of development (right). The GFP-cFIP-expressing cells form fruiting bodies that are reduced in size by 30% compared with the AX2 cells. The columns represent mean±s.e. value [t_8: n=268 (GFP-cFIP), 270 (AX2); t_{24}: n=96 (GFP-cFIP), 41 (AX2)]. The experiments were performed three times. (C) AX2 cells expressing GFP-cFIP have a phototaxis defect. Slugs do not move straight towards the light but at an angle and travel shorter distances. (a) Behavior of AX2 wild-type slugs, (b), behavior of GFP-cFIP-expressing AX2 slugs. Slug migration was for 48 hours. The location of the light source is indicated by an arrowhead.

we tested the phototaxis behavior of AX2 cells expressing GFP-cFIP. The cells were able to form migrating slugs. However, they differed in comparison with wild-type slugs in two respects. Wild-type slugs migrate almost directly towards a lateral light source. Slugs expressing GFP-cFIP resemble the filamin-deficient strains GHR and HG1264 in their phototactic behavior. They do not orient properly and do not migrate as far as wild-type slugs in the same period of time (Fig. 8C).

Discussion

A novel filamin-interacting protein has α-helical coiled coil domains

Elucidating the interaction partners of filamin is crucial to our understanding of the molecular mechanisms that regulate the diverse cellular functions of this actin-cytoskeleton-associated protein. Findings from interaction studies with vertebrate filamins indicate an involvement of the filamin protein family in such diverse processes as mechanical stability, intracellular trafficking and signal transduction (Stossel et al., 2001; Stossel and Hartwig, 2003).

Using a yeast two-hybrid screen, we have identified a novel protein, FIP, that interacts with the elongated domain of *Dictyostelium* filamin. FIP is a so-far-unknown protein with 2038 amino acids. It has a high overall content of α-helical structure and two central α-helical coiled coil domains can be defined. FIP does not contain transmembrane, nuclear localization, or other signal peptide motifs. Database searches for homologous proteins revealed about 20% identity to proteins with coiled coil domains like interaptin (Rivero et al., 1998). The regions of similarity correspond to the proposed coiled coil domains. The intracellular distribution of FIP and the property of the C-terminus to localize to the plasma membrane suggest that FIP can associate with membranes. On the basis of the presence of the coiled coil regions as well as the leucine zipper, it has the potential to form an interaction surface for several proteins that assemble at membranes (Burkhard et al., 2001). One of these is filamin, which can provide a link to the actin cytoskeleton and render the distribution of FIP susceptible to treatments by agents that disturb the actin cytoskeleton.

It is interesting to note that several of the homologous coiled coil proteins are associated with membranes. Interaptin, a developmentally regulated member of the spectrin superfamily

of actin-binding proteins in *D. discoideum* with an extended central coiled coil domain, localizes to the cytoplasmic site of the endoplasmic reticulum (Rivero et al., 1998). Golgin-245, originally identified as a member of a family of self-antigens recognized by autoantisera from patients with Sjögrens syndrome (Fritzler et al., 1995; Erlich et al., 1996; Griffith et al., 1997), is a large protein predicted to form extensive α-helical coiled coils and is located at the cytoplasmic face of Golgi membranes and Golgi-derived vesicles. In fractionation experiments with yeast cells expressing a GFP fusion of the yeast golgin-related protein Imh1p, a portion of the chimeric protein remained in the cytosolic supernatant, and the other portion pelleted with the membrane fraction that contained vesicles and the Golgi apparatus. This is consistent with a peripheral membrane association (Munro and Nichols, 1999).

FIP has a function in the development of *Dictyostelium*

The contribution of cytoskeletal proteins in the developmental program of *Dictyostelium* has been well established by mutant analysis. The cytoskeletal proteins themselves are in general not strongly regulated during development although exceptions exist (Noegel and Luna, 1995; Gloss et al., 2003). Filamin is expressed in nearly equal amounts during growth and development. Therefore, the filamin functions during development established by mutant analysis, such as reduced chemotactic efficiency in response to cAMP (Cox et al., 1992) and impaired photo- and thermosensory responses of the slug (Fisher et al., 1997), may be regulated by the expression of filamin interaction partners involved in these processes. For this, FIP is a likely candidate, because mRNA transcript and protein levels are very low in growing cells, but are present at high levels from the early stages of development to the formation of the fruiting body.

Since we were not successful in our attempts to isolate a mutant deficient for FIP, we studied the consequences of GFP-cFIP expression in wild-type cells and found that it led to a more rapid development. Premature development has been observed in several *Dictyostelium* mutants. In general, these mutants are deficient in components of the cAMP signaling system such as the regulatory subunit of protein kinase A (PKA) or a phosphodiesterase, or they overexpress components such as Dd PK2, a homolog of PKA (Kim et al., 1998; Anjard et al., 1992). Deletion of the gene coding for the regulatory subunit of PKA, which releases the catalytic subunit from inhibition, also causes development to proceed very rapidly (Abe and Yanagisawa, 1983; Simon et al., 1992). By contrast, deletion of the catalytic subunit of the PKA leads to an aggregateless phenotype (Mann et al., 1997; Wu et al., 1995).

The most important alteration that connects FIP to filamin was the defect in phototaxis. Like filamin-deficient mutants, the GFP-cFIP-expressing strain had a comparable impairment in phototaxis. The slugs migrated less distance and did not orient properly towards the light. These results point towards an involvement of FIP in processes ensuring correct development and phototaxis and make it a good candidate to support filamin in its role during specific developmental stages.

We thank R. Müller for generation and purification of the filamin polypeptides and carrying out the interaction and immunoprecipitation experiments, R. Blau-Wasser for performing immunofluorescence studies, B. Gassen for assistance with the preparation of monoclonal antibodies and B. Lauss for organizing the manuscript. We are grateful to F. Rivero for help in the use of the confocal microscope, and to our colleagues M. Mohrs and A. Lautwein for helpful discussions. This work was supported by grants from the Deutsche Forschungsgemeinschaft, the Fonds der Chemischen Industrie and Köln Fortune.

References

Abe, K. and Yanagisawa, K. (1983). A new class of rapid developing mutants in *Dictyostelium discoideum*: implications for cyclic AMP metabolism and cell differentiation. *Dev. Biol.* **95**, 200-210.

Anjard, C., Pinaud, S., Kay, R. R. and Reymond, C. D. (1992). Overexpression of Dd PK2 protein kinase causes rapid development and affects the intracellular cAMP pathway of *Dictyostelium discoideum*. *Development* **115**, 785-790.

Ayscough, K. R. (1998). In vivo functions of actin-binding proteins. *Curr. Opin. Cell Biol.* **10**, 102-111.

Brink, M., Gerisch, G., Isenberg, G., Noegel, A. A., Segall, J. E., Wallraff, E. and Schleicher, M. (1990). A *Dictyostelium* mutant lacking an F-actin cross-linking protein, the 120-kD gelation factor. *J. Cell Biol.* **97**, 178-185.

Burkhard, P., Stetefeld, J. and Strelkov, S. V. (2001). Coiled coils: a highly versatile protein folding motif. *Trends Cell Biol.* **11**, 82-88.

Claviez, M., Pagh, K., Maruta, H., Baltes, W., Fisher, P. and Gerisch, G. (1982). Electron microscopic imaging of monoclonal antibodies on the tail region of *Dictyostelium* myosin. *EMBO J.* **1**, 1017-1022.

Cox, D., Condeelis, J., Wessels, D., Soll, D., Kern, H. and Knecht, D. A. (1992). Targeted disruption of the ABP-120 gene leads to cells with altered motility. *J. Cell Biol.* **116**, 943-955.

Cox, D., Rinsdale, J. A., Condeelis, J. and Hartwig, J. (1995). Genetic deletion of ABP-120 alters the three-dimentional organization of actin filaments in *Dictyostelium* pseudopods. *J. Cell Biol.* **128**, 819-835.

Cox, D., Wessels, D., Soll, D. R., Hartwig, J. and Condeelis, J. (1996). Re-expression of ABP-120 rescues cytoskeletal, motility and phagocytosis defects of ABP-120^{-} *Dictyostelium* mutants. *Mol. Biol. Cell* **7**, 803-823.

Devreotes, P. N. and. Zigmond, S. H. (1988). Chemotaxis in eucaryotic cells: a focus on leukocytes and *Dictyostelium*. *Annu. Rev. Cell Biol.* **4**, 649-686.

Durfee, T., Becherer, K., Chen, P. L., Yeh, S. H., Yang, Y., Kilburn, A. E., Lee, W. H. and Elledge, S. J. (1993). The retinoblastoma protein associates with the protein phosphatase type 1 catalytic subunit. *Genes Dev.* **7**, 555-569.

Eichinger, L. and Schleicher, M. (1992). Characterization of actin- and lipid-binding domains in severin, a Ca(2+)-dependent F-actin fragmenting protein. *Biochemistry* **31**, 4779-4787.

Erlich, R., Campbell, P. A., Dietzsch, E. and Toh, B. H. (1996). Molecular characterization of *trans*-Golgi p230. A human peripheral membrane protein encoded by a gene on chromosome 6p12-22 contains extensive coiled-coil α-helical domains and a granin motif. *J. Biol. Chem.* **271**, 8328-8337.

Fisher, P. R., Noegel, A. A., Fechheimer, M., Rivero, F., Prassler, J. and Gerisch, G. (1997). Photosensory and thermosensory responses in *Dictyostelium* slugs are specifically impaired by absence of the F-actin cross-linking gelation factor (ABP-120). *Curr. Biol.* **7**, 889-892.

Fritzler, M. J., Lung, C. C., Hamel, J. C., Griffith, K. J. and Chan, E. K. L. (1995). Molecular characterization of golgin-245, a novel Golgi complex protein containing a granin signature. *J. Biol. Chem.* **270**, 31262-31268.

Fucini, P., Renner, C., Herberhold, C., Noegel, A. A. and Holak, T. (1997). The repeating segments of the F-actin crosslinking gelation factor (ABP-120) have an immunoglobulin-like fold. *Nat. Struct. Biol.* **4**, 223-230.

Fucini, P., Köppel, B., Schleicher, M., Lustig, A., Holak, T., Müller, R., Stewart, M. and Noegel, A. A. (1999). Molecular architecture of the rod domain of the *Dictyostelium* gelation factor (ABP120). *J. Mol. Biol.* **291**, 1017-1023.

Gloss, A., Rivero, F., Khaire, N., Müller, R., Loomis, W. F., Schleicher, M. and Noegel, A. A. (2003). Villidin, a novel WD-repeat and villin-related protein from *Dictyostelium*, is associated with membranes and the cytoskeleton. *Mol. Biol. Cell* **14**, 2716-2727.

Gietz, R. D. and Schiestl, R. H. (1995). Transforming yeast with DNA. *Methods Mol. Cell. Biol.* **5**, 255-269.

Gorlin, J. B., Yamin, R., Egan, S., Stewart, M., Stossel, T. P., Kwiatkowski, D. J. and Hartwig, J. H. (1990). Human endothelial actin-binding protein (ABP-280, nonmuscle filamin): a molecular leaf spring. *J. Cell Biol.* **111**, 1089-1105.

Griffith, K. J., Chan, E. K. L., Lung, C. C., Hamel, J. C., Guo, X. Y., Miyachi, K. and Fritzler, M. J. (1997). Molecular cloning of a novel 97-kd Golgi complex autoantigen associated with Sjögren's syndrome. *Arthritis Rheum.* **40**, 1693-1702.

Hartwig, J. (1994). Spectrin superfamily. In *Protein Profile* (ed. P. Shelterline), pp. 711-778. London, UK: Academic Press.

He, H. J., Kole, S., Kwon, Y. K. and Bernier, M. (2003). Interaction of filamin A with the insulin receptor alters insulin-dependent activation of the mitogen-activated protein kinase pathway. *J. Biol. Chem.* **278**, 27096-27104.

Jungbluth, A., von Armin, V., Biegelmann, B., Humbel, B., Schweiger, A. and Gerisch, G. (1994). Strong increase in the tyrosine phosphorylation of actin upon inhibition of oxidative phosphorylation: correlation with reversible rearrangements in the actin skeleton of *Dictyostelium* cells. *J. Cell Sci.* **107**, 117-125.

Kim, H. J., Chang, W. T., Meima, M., Gross, J. D. and Schaap, P. (1998). A novel adenylyl cyclase detected in rapidly developing mutants of *Dictyostelium*. *J. Biol. Chem.* **273**, 30859-30862.

Laemmli, U. K. (1970). Cleavage of structural proteins during the assembly of the head of bacteriophage T4. *Nature* **227**, 722-725.

Lin, R., Canfield, V. and Levenson, R. (2002). Dominant negative mutants of filamin A block cell surface expression of the D2 dopamine receptor. *Pharmacology* **66**, 173-181.

Loy, C. J., Sim, K. S. and Yong, E. L. (2003). Filamin-A fragment localizes to the nucleus to regulate androgen receptor and coactivator functions. *Proc. Natl. Acad. Sci. USA* **100**, 4562-4567.

Lupas, A., van Dyke, M. and Stock, J. (1991). Predicting coiled coils from protein sequences. *Science* **252**, 1162-1164.

Mann, S. K. O., Brown, J. M., Briscoe, C., Parent, C., Pitt, G., Devreotes, P. N. and Firtel, R. A. (1997). Role of cAMP-dependent protein kinase in controlling aggregation and postaggregative development in *Dictyostelium*. *Dev. Biol.* **183**, 208-221.

Marti, A., Luo, Z., Cunningham, C., Otha, Y., Hartwig, J., Stossel, T. P., Kyriakis, J. M. and Avruch, J. (1997). Actin-binding protein-280 binds the stress-activated protein kinase (SAPK) activator SEK-1 and is required for tumor necrosis factor-alpha activation of SAPK in melanoma cells. *J. Biol. Chem.* **272**, 2620-2628.

McCoy, A. J., Fucini, P., Noegel, A. A. and Stewart, M. (1999). Structural basis for dimerisation of the *Dictyostelium* gelation factor (ABP120) rod. *Nat. Struct. Biol.* **6**, 836-841.

Munro, S. and Nichols, B. J. (1999). The GRIP domain – a novel Golgi-targeting domain found in several coiled-coil proteins. *Curr. Biol.* **9**, 377-380.

Nakajima, H., Hirata, A., Ogawa, Y., Yonehara, T., Yoda, K. and Yamasaki, M. (1991). A cytoskeleton-related gene, iso1, is required for intracellular protein transport in *Saccharomyces cerevisiae*. *J. Cell Biol.* **113**, 245-260.

Newell, P. C., Telser, A. and Sussman, M. (1969). Alternative developmental pathways determined by environmental conditions in the cellular slime mold *Dictyostelium discoideum*. *J. Bacteriol.* **100**, 763-768.

Noegel, A. A. and Luna, J. E. (1995). The *Dictyostelium* cytoskeleton. *Experientia* **51**, 1135-1143.

Noegel, A. A., Metz, B. A. and Williams, K. L. (1985). Developmentally regulated transcription of *Dictyostelium discoideum* plasmid Ddp1. *EMBO J.* **4**, 3797-3803.

Noegel, A. A., Rapp, S., Lottspeich, F., Schleicher, M. and Stewart, M. (1989). The *Dictyostelium* gelation factor shares a putative actin binding site with α-actinins and dystrophin and also has a rod domain containing six 100-residue motifs that appear to have a cross-beta conformation. *J. Cell Biol.* **109**, 607-618.

Noegel, A. A., Rivero, F., Fucini, P., Bracco, E., Janssen, K. P. and Schleicher, M. (1997). Actin binding proteins: role and regulation. In *Dictyostelium. A Model System for Cell and Developmental Biology* (ed. Y. Maeda, K. Inouye and I. Takeuchi), pp. 33-42. Tokyo, Japan: Universal Academy Press.

Noegel, A. A., Blau-Wasser, R., Sultana, H., Israel, L., Schleicher, M., Patel, H. and Weijer, C. J. (2004). CAP/ASP56 as regulator of cell polarity and cAMP signaling in *Dictyostelium*. *Mol. Biol. Cell* **15**, 934-945.

Otha, Y., Suzuki, N., Nakamura, S., Hartwig, J. and Stossel, T. P. (1999). The small GTPase RalA targets filamin to induce filopodia. *Proc. Natl. Acad. Sci. USA* **96**, 2122-2128.

Rivero, F., Kuspa, A., Brokamp, R., Matzner, M. and Noegel, A. A. (1998). Interaptin, an actin-binding protein of the α-actinin superfamily in *Dictyostelium discoideum*, is developmentally and cAMP-regulated and associates with intracellular membrane compartments. *J. Cell Biol.* **142**, 735-750.

Simon, M. N., Pelegrini, O., Véron, M. and Kay, R. R. (1992). Mutation of protein kinase-A causes heterchronic development of *Dictyostelium*. *Nature* **356**, 171-172.

Simpson, P. A., Spudich, J. A. and Parham, P. (1984). Monoclonal antibodies prepared against *Dictyostelium* actin: characterisation and interactions with actin. *J. Cell Biol.* **99**, 287-295.

Stahlhut, M. and van Deurs, B. (2000). Identification of filamin as a novel ligand for caveolin-1: evidence for the organization of caveolin-1-associated membrane domains by the actin cytoskeleton. *Mol. Biol. Cell* **11**, 325-337.

Stossel, T. P. and Hartwig, J. H. (2003). Filling gaps in signaling to actin cytoskeletal remodeling. *Dev. Cell* **4**, 444-445.

Stossel, T. P., Condeelis, J., Cooley, L., Hartwig, J. H., Noegel, A., Schleicher, M. and Shapiro, S. S. (2001). Filamins as integrators of cell mechanics and signalling. *Nat. Rev. Mol. Cell Biol.* **2**, 138-145.

Tabor, S. and Richardson, C. C. (1992). A bacteriophage T7 RNA polymerase/promotor system for controlled exclusive expression of specific genes. *Biotechnology* **24**, 280-284.

Towbin, H., Staehelin, T. and Gordon, J. (1979). Electrophoretic transfer of proteins from polyacrylamide gels to nitrocellulose sheets: procedure and some applications. *Proc. Natl. Acad. Sci. USA* **76**, 4350-4354.

Tu, Y., Wu, S., Shi, X., Chen, K. and Wu, C. (2003). Migfilin and Mig-2 link focal adhesions to filamin and the actin cytoskeleton and function in cell shape modulation. *Cell* **113**, 37-47.

Wallraff, E. and Wallraff, H. G. (1997). Migration and bidirectional phototaxis in *Dictyostelium discoideum* slugs lacking the actin cross-linking 120 kDa gelation factor. *J. Exp. Biol.* **200**, 3213-3220.

Weiner, O. H., Murphy, J., Griffiths, G., Schleicher, M. and Noegel, A. A. (1993). The actin-binding protein comitin (p24) is a component of the Golgi apparatus. *J. Cell Biol.* **123**, 23-34.

Westphal, M., Jungbluth, A., Heidecker, M., Mühlbauer, B., Heizer, C., Schwartz, J.-M., Marriot, G. and Gerisch, G. (1997). Microfilament dynamics during cell movement and chemotaxis monitored using a GFP-actin fusion. *Curr. Biol.* **7**, 176-183.

Williams, K. L. and Newell, P. C. (1976). A genetic study in the cellular slime mold *Dictyostelium discoideum* using complementation analysis. *Genetics* **82**, 287-307.

Wu, L., Hansen, D., Franke, J., Kessin, R. H. and Podgorski, G. J. (1995). Regulation of *Dictyostelium* early developmental genes in signal transduction mutants. *Dev. Biol.* **171**, 149-158.